Received: 22 January 2021 | Revised: 15 November 2021 | Accepted: 30 December 2021

DOI: 10.1002/sia.7067

RESEARCH ARTICLE

SURFACE and INTERFACE ANALYSIS WILEY

A structural analysis of ultrathin barrier (In)AlN/GaN heterostructures for GaN-based high-frequency power electronics

Polat Narin[1,2] | Ece Kutlu-Narin[1,3] | Gokhan Atmaca[1] | Beyza Sarikavak-Lisesivdin[1] | Sefer B. Lisesivdin[1] | Ekmel Ozbay[4,5,6]

[1]Department of Physics, Faculty of Science, Gazi University, Ankara, Turkey

[2]Central Research Laboratory Application and Research Center, Ankara Yıldırım Beyazıt University, Ankara, Turkey

[3]Department of Physics Engineering, Faculty of Engineering, Ankara University, Ankara, Turkey

[4]Nanotechnology Research Center, Bilkent University, Ankara, Turkey

[5]Department of Physics, Bilkent University, Ankara, Turkey

[6]Department of Electrical and Electronics Engineering, Bilkent University, Ankara, Turkey

Correspondence
Polat Narin, Central Research Laboratory Application and Research Center, Ankara Yıldırım Beyazıt University, Ankara 06050, Turkey.
Email: pnarin@ybu.edu.tr

Funding information
Turkish Academy of Sciences, Grant/Award Number: TUBA-GEBIP 2016

Metal–organic chemical vapor deposition (MOCVD) is one of the best growth methods for GaN-based materials as well-known. GaN-based materials with very quality are grown the MOCVD, so we used this growth technique to grow InAlN/GaN and AlN/GaN heterostructures in this study. The structural and surface properties of ultrathin barrier AlN/GaN and InAlN/GaN heterostructures are studied by X-ray diffraction (XRD) and atomic force microscopy (AFM) measurements. Screw, edge, and total dislocation densities for the grown samples have been calculated by using XRD results. The lowest dislocation density is found to be 1.69×10^8 cm^{-2} for Sample B with a lattice-matched $In_{0.17}Al_{0.83}N$ barrier. The crystal quality of the studied samples is determined using (002) symmetric and (102) asymmetric diffractions of the GaN material. In terms of the surface roughness, although reference sample has a lower value as 0.27 nm of root mean square values (RMS), Sample A with 4-nm AlN barrier layer exhibits the highest rough surface as 1.52 nm of RMS. The structural quality of the studied samples is significantly affected by the barrier layer thickness. The obtained structural properties of the samples are very important for potential applications like high-electron mobility transistors (HEMTs).

KEYWORDS
AFM, GaN, structural properties, ultrathin, XRD

1 | INTRODUCTION

Gallium nitride (GaN)-based heterostructures have been investigated for many years due to their ability to work in both high frequencies and high temperatures (HTs).[1–3] Because GaN-based materials are in the wurtzite structure, the heterostructures built with these materials have piezoelectric polarization-induced electric field due to strain between the layers in structure, and each layer has its own spontaneous polarization-induced electric field.[4,5] These polarization-induced electric fields lead GaN-based heterostructures are used in some electronic and optoelectronic devices such as high-electron mobility transistors (HEMTs) and light-emitting diodes (LEDs).[6,7] In GaN-based heterostructures, many different barrier layer types with different materials and thicknesses can be grown on GaN buffer. These different materials might be an alloy such as AlGaN and AlInN or might be a binary semiconductor as AlN and InN.[8–10] Besides different materials, the layer thickness of the barriers is also important. High-frequency GaN devices used in the industry typically suffer from short-channel effect due to the poor aspect ratio. This issue is caused by the strain relaxation issues that limit the AlGaN content to less than 40%. Due to the effects of the recess gate technique on high-frequency GaN transistor's performance, it is commonly used to avoid the use of chemical etching. A new approach that uses Al-rich ultrathin barrier layer can help minimize the effects of the recess gate technique and increase the performance and reliability of GaN devices. The structures with the barrier layer thicknesses lower than 7 nm are classified as ultrathin barrier HEMTs.[11,12]

Ostermaier et al. proposed an ultrathin barrier GaN-based heterostructure with a 1-nm InAlN barrier layer and 1-nm AlN interlayer and 6-nm highly doped GaN cap layer.[13] This ultrathin barrier structure has many important features such as observing the short-channel effect and high transconductance in a HEMT structure.[14] Importantly, in addition to highly used AlGaN barrier layers, the InAlN barrier layer can be grown as lattice matched with the GaN buffer layer only for 17%–18% of In mole fraction. The possible structural dislocations causing lattice mismatch may be eliminated owing to the strained barrier layer.

During the growth process of a crystal, unwanted defects, dislocations, and strain may have occurred. The dislocations in a crystal and other structural parameters such as the thickness, the alloy mole fraction, the lattice parameters can be calculated by X-ray diffraction (XRD) results, which is nondestructive method.[5,15–18] To investigate the dislocation densities that include edge and screw types in terms of the structural quality is important, because the dislocations are one of the main effects that deteriorate the device performance of the HEMTs.[19–21] One of the main reasons for the dislocations is the strain relaxation that occurred at the interfaces. The detailed investigation of the dislocations and the possible strain relaxation will provide a better understanding of the ultrathin barrier HEMTs that are very vulnerable to change in strain.

From morphological analysis, surface problems such as crack, dislocations etc. could be determined. In general, AFM measurement is used to show these morphological defects.[22] The surface analysis is important in terms of GaN-based device performance because these defects in structure can be formed locally charge centers, which is negatively affected the HEMTs.[23,24]

In literature, GaN-based materials are grown using MOCVD and molecular beam epitaxy (MBE) system. Especially, compared with MBE systems, MOCVD has some advantages such as high growth rate, mass production, or growth on more than one substrates.[25] Also, because of higher growth rate of MOCVD, it is possible to use the commercial applications.[26] Generally, GaN-based HEMT structures are grown on the sapphire (Al_2O_3) due to the low cost of sapphire and the high cost of bulk GaN substrates. The lattice mismatch between the chosen buffer layer and the sapphire substrate causes high densities of dislocations in the growths.[27] Over the past years, researchers have proposed the usage of AlN nucleation layer that is grown in the low temperature (LT) between GaN and sapphire to eliminate the lattice mismatch.[28,29] In the next step to increase the crystal quality, AlN buffer layer that is grown at HT has been proposed.[30–32] In this study, the structural properties of ultrathin barrier AlN/GaN and InAlN/GaN HEMT structures that are grown by MOCVD have been investigated by using the XRD and atomic force microscopy (AFM) measurements. For each studied structure, the lattice parameters, the dislocation densities, and the surface morphologies have been calculated in detail.

2 | EXPERIMENTAL TECHNIQUES

Ultrathin barrier AlN/GaN and $In_{0.17}Al_{0.83}N$/GaN heterostructures were identically grown in a low-pressure MOCVD reactor (Aixtron 200/4 HT-S) on c-face (0001) sapphire substrates by using trimethylaluminum (Nouryon Products, Amsterdam), trimethylgallium (Nouryon Products, Amsterdam), trimethylindium (Nouryon Products, Amsterdam), silane (Linde Gas, Ankara), and ammonia (Linde Gas, Ankara) as Al, Ga, In, Si, and N precursors, respectively. Firstly, the substrate surface was annealed for 10 min in H_2 ambient at 1050°C to provide the substrate surface clean. After the substrate cleaning, the 15-nm AlN nucleation layer was grown at an LT of 770°C to increase the lattice match between GaN and sapphire. AlN buffer layer with 300-nm thickness was grown on the AlN nucleation layer at a HT of 1180°C. In the next step, about ~1.3-μm undoped GaN layer was grown at 1100°C. A reference sample was grown with an about ~1-nm AlN interlayer at HT of 1130°C. The barrier layers of the A, B, C, and reference sample structures were grown undoped 4-nm AlN at 1120°C, undoped 3-nm $In_{0.17}Al_{0.83}N$ at 830°C, 1×10^{19} cm^{-3} Si-doped 3-nm AlN at 1100°C and undoped 1-nm $In_{0.17}Al_{0.83}N$ at 890°C, respectively. For all of the samples, the cap layers were grown at 830°C. The cap layer thicknesses of A, B, C, and reference sample structures are undoped 1-nm GaN, 1×10^{20} cm^{-3} Si-doped 2-nm GaN, undoped 2-nm GaN, and 1×10^{20} cm^{-3} Si-doped 6-nm GaN, respectively. To form Si-doped layers, silane (SiH_4) was used.

The effect of different barrier layers with different thicknesses, doping rates, and cap layer thicknesses on crystal quality is investigated in this study. The crystal quality and structural parameters of the grown heterostructures are determined by using XRD measurements. Rikagu SmartLab diffractometer, which is equipped with four crystals Ge (220) monochromator, was used to provide $CuK_{\alpha 1}$ X-ray beam ($\lambda = 0.154$ nm). Symmetric (002) and asymmetric (102) diffractions of GaN layers were measured out. AFM measurements were carried out by Veeco DI-CP II system using contact mode on 4.6×4.6 μm^2 scan size of samples.

3 | RESULTS AND DISCUSSION

The investigated GaN-based heterostructures have two different barrier structure as AlN and InAlN. The GaN-based heterostructures have different barrier and cap layers. The structural and morphological properties of these structures are presented in this section with the results of XRD and AFM measurements. The structural represantation of the studied samples is shown in Figure 1. The barrier regions of the prepared structures have different layer structures as shown in Figure 1.

Figure 2 shows (0002) the diffraction patterns of the studied ultrathin AlN/GaN and $In_{0.17}Al_{0.83}N$/GaN structures that have different barriers and thicknesses. AlN and GaN peaks are only shown; the diffraction peak of the InAlN barrier layer is not obtained because of its ultrathin thickness.[33] The (002) diffractions of GaN and AlN materials of the reference sample are shifted to lower diffraction angles due to compressive strain in structure. As it is widely known, the AlN interlayer reduces alloy scattering of the mobility of two-dimensional electron gas (2DEG), but in most cases, it may bring additional

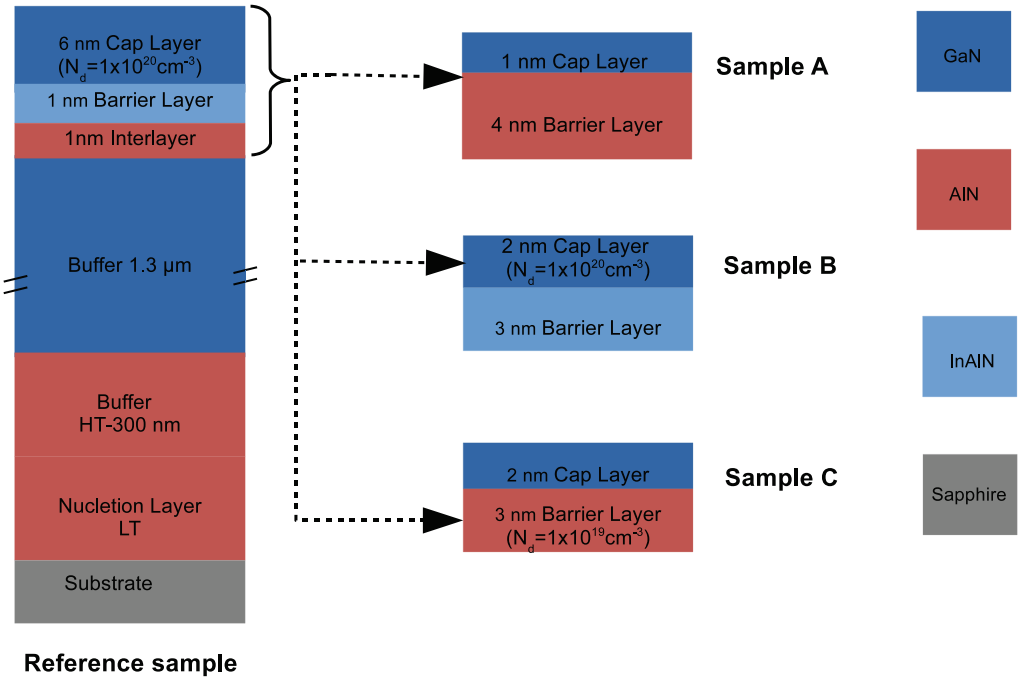

FIGURE 1 The layer structure of the reference, A, B, and C samples

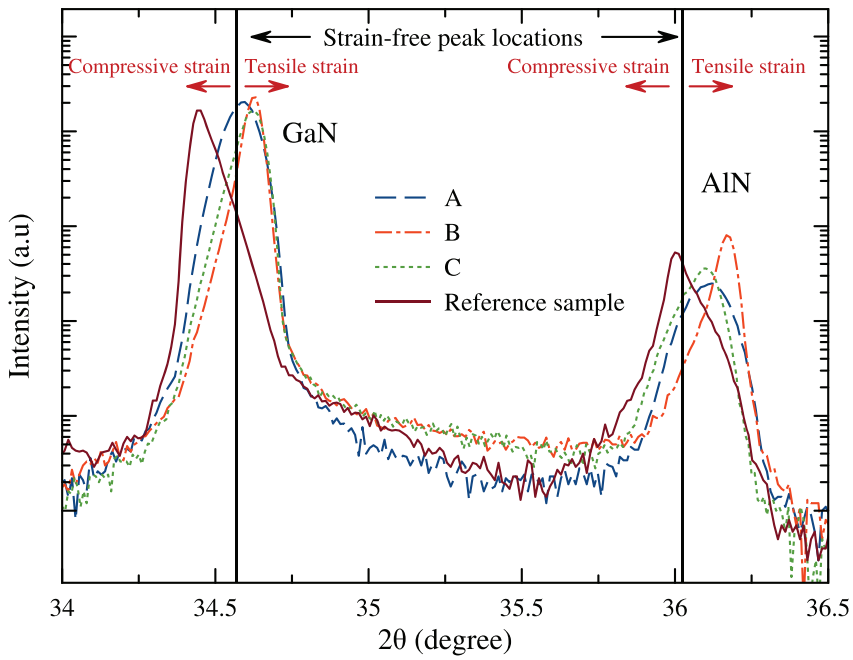

FIGURE 2 X-ray diffraction (XRD) patterns of Sample A, B, C, and the reference sample

compressive strain to the lattice.[34–36] Other samples show a tensile strain structure. Also, the quality of the structure can be determined by comparing the width of the peaks. Hence, the structural quality of Sample B can be accepted to be the best. For more detailed structural analysis, the symmetric (002) and the asymmetric (102) reflection peaks of GaN material are analyzed. Figures 3 and 4 show the related reflections of the studied samples. As seen in Figure 3, the most narrow peak is observed for Sample B. Samples A and C have wider peaks. In Figure 4, the reflection of asymmetric (102) scans of the GaN layer for Samples A, B, C, and reference sample structures are shown. As expected, (102) asymmetric reflection of the GaN material shows peaks with a wider full width at half maximum (FWHM) values as compared with (002) symmetric scan of the GaN layer. In (102), whereas FWHM values of Samples B and C are lower than the literature values of 0.069°–0.083° for GaN (002) and 0.084°–0.097° for GaN (102), Sample A is higher than these values.[28,30] Also, the reference sample is in the ranges with these values. FWHM values for (002) symmetric reflection of Samples B and C are found to be better

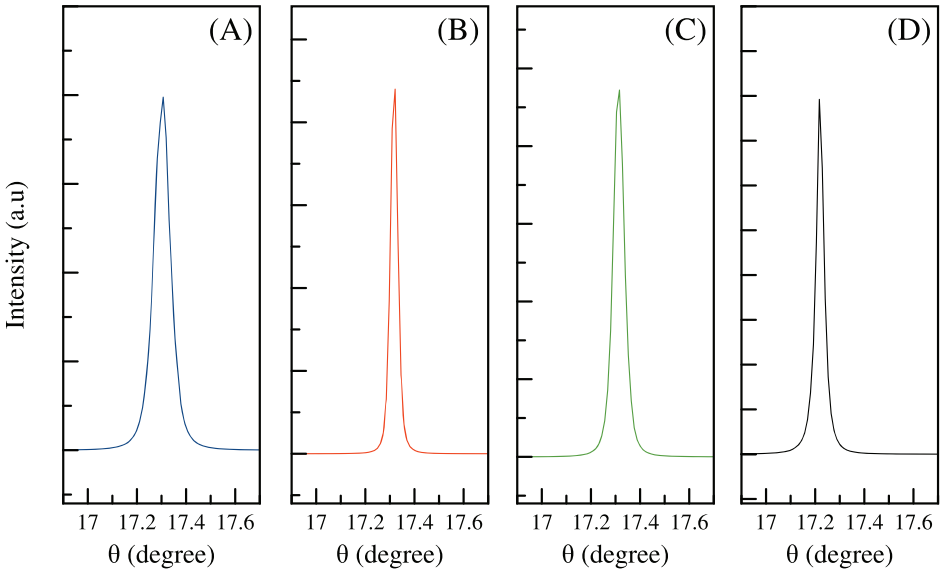

FIGURE 3 Reflection of (002) symmetric scan of the GaN layer for Samples (A) A, (B) B, (C) C, and (D) the reference sample

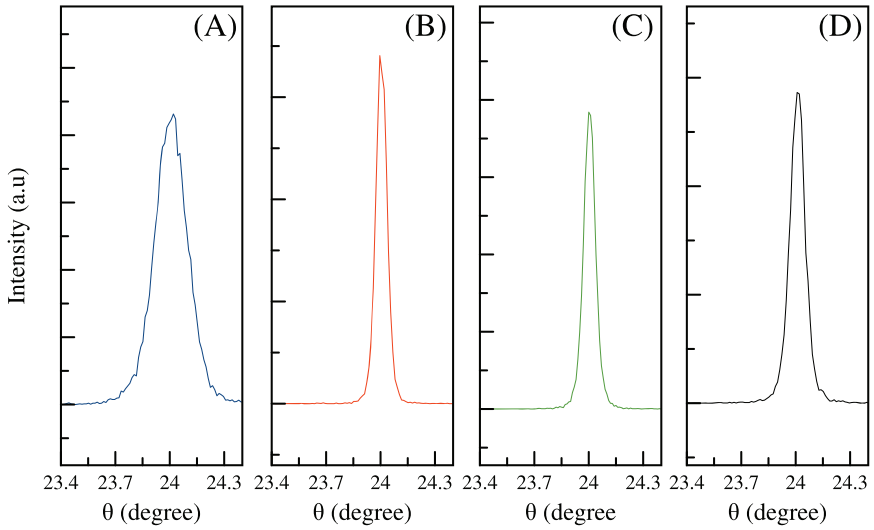

FIGURE 4 Reflection of (102) asymmetric scan of the GaN material for Samples (A) A, (B) B, (C) C, and (D) reference sample

than the literature values. FWHM values for both symmetric (002) and asymmetric (102) reflections of the GaN material are given in Table 1.

$$\frac{1}{d_{hkl}^2}=\frac{4}{3}\left(\frac{h^2+hk+k^2}{a^2}\right)+\frac{l^2}{c^2}, \tag{1}$$

$$\varepsilon_{zz}=\frac{(c-c_0)}{c_0}. \tag{2}$$

Dislocation densities in these samples are calculated using

$$N_{screw}=\frac{FWHM_{(002)}^2}{4.35b_{screw}^2}, \tag{3}$$

$$N_{edge}=\frac{FWHM_{(102)}^2}{4.35b_{edge}^2}, \tag{4}$$

and

$$N_{tot}=N_{screw}+N_{edge}. \tag{5}$$

Here, N_{screw}, N_{edge}, N_{tot}, b_{screw}, and b_{edge} are dislocation densities for screw dislocation, edge dislocation, the sum of the screw and the edge dislocations, the Burger vectors length of the screw, and the edge dislocations, respectively.[37] The structural quality of the studied structures is related to dislocation density. Also, it is known that the electrical properties, especially electron mobility of 2DEG in these structures, are negatively affected by the increasing dislocation density.[38] The calculated dislocation density values of each sample have been given in Table 2. It is shown that Sample A has the highest

TABLE 1 Lattice and strain parameters for GaN and AlN layers

Parameters	Sample A	Sample B	Sample C	Reference sample	Other studies[28,30,41,42]
c (Å)					
GaN	5.182	5.176	5.178	5.203	5.183, 5.186 5.189
AlN	4.969	4.963	4.972	4.985	4.980, 4.979, 4.982
Strain (ε_{zz})					
GaN	−0.0007	−0.0019	−0.0015	0.0032	
AlN	−0.0022	−0.0034	−0.0016	0.0010	

TABLE 2 FWHM values and X-ray diffraction (XRD) peaks angles of (002) symmetric and (102) asymmetric reflections of the GaN layer for reference sample and Samples A, B, and C

Parameters	Sample A	Sample B	Sample C	Reference sample
FWHM (°)				
(002)	0.084	0.036	0.053	0.078
(102)	0.209	0.072	0.072	0.094
XRD peaks (°)				
(002)	17.316	17.321	17.316	17.228
(102)	24.020	23.996	24.000	24.008

Abbreviations: FWHM, full width at half maximum; XRD, X-ray diffraction.

dislocation density and Sample B has the lowest dislocation density. Besides, the edge dislocation density of Sample A is higher than other samples about 10 times due to (102) asymmetry reflection of its.

Possible dislocation formation can be guessed by the thickness of barrier layers exceed or not the critical thickness where the strain between the related two layers is relaxed and the dislocations formed. The critical thickness can be calculated with

$$t_c \cong \frac{b_e}{2\varepsilon_x}. \quad (6)$$

Here, b_e and ε_x are the Burger vector length and biaxial strain, respectively. In Table 3 is shown the calculated critical with Equation 4 and grown thicknesses of the barrier layer for each sample. If barrier layer thickness close to the critical thickness, then some can expect an increment in the dislocation density due to increased strain in the structure.[9] As the barrier layer thickness of Sample A is closer to critical thickness than Sample C, the dislocation density of Sample A is higher than Sample C. At the same time, the dislocation density of the reference sample due to about 1-nm AlN interlayer is higher as compared with Sample B.

As AlN barrier thickness close to critical thickness, it is known that strain is higher and even strain relaxation will be occurred in AlN/GaN heterostructures depending on growth conditions. If the strain between the layers increases in a HEMT structure with an ultrathin barrier, then it can be expected that roughness will take form at the surface of the structure due to this strained part that is occurred very near to surface.

The root mean square values (RMS) of the lateral correlation length (Λ) and the amplitude (Δ) of roughness are determined in Figure 5 by AFM images and surface profiles which is the scanning area of 4.6 × 4.6 μm^2. The surface of the reference sample is very smooth in comparison with other samples. Because the thickness of the AlN barrier layer of Sample A is closer than Sample C to the critical thickness according to Table 4, a strain relaxation or a highly strained structure can be expected for Sample A. From the surface profile of Sample A, the roughness amplitude of the RMS value is higher than other samples. It is well known that, in a HEMT structure, such roughness amplitude value leads to a dominant roughness scattering mechanism on 2DEG at the heterointerface.[39] Therefore, the electrical results of Sample A may be shown poorer compared with the other samples. Because Samples B and reference are grown as lattice matched, both samples have a lower RMS of surface roughness for Sample A; longer lateral correlation lengths are observed, while other samples have similar behavior. According to RMS of roughness amplitude results, the surfaces of Samples reference and B can be accepted as smooth. The calculated dislocation densities from XRD result are consistent with AFM result according to RMS values of the samples. Sample A with the highest dislocation density has a highest rough surface with 1.52 nm of RMS. Also, Samples reference, B, and C have the step-like characteristics in some areas of surfaces shown best in Figure 5. Moreover, our previous results related to these samples show that the reference sample has the highest 2DEG mobility among these samples at LT by Hall effect measurements.[40]

TABLE 3 Calculated edge, screw, and total dislocation densities of the reference, A, B, and C samples

Sample	N_{edge} (cm^{-2})	N_{screw} (cm^{-2})	N_{tot} (cm^{-2})
A	1.14×10^9	1.84×10^8	1.32×10^9
B	1.35×10^8	3.37×10^7	1.69×10^8
C	1.35×10^8	7.31×10^7	2.08×10^8
Reference	2.30×10^8	1.58×10^8	3.88×10^8

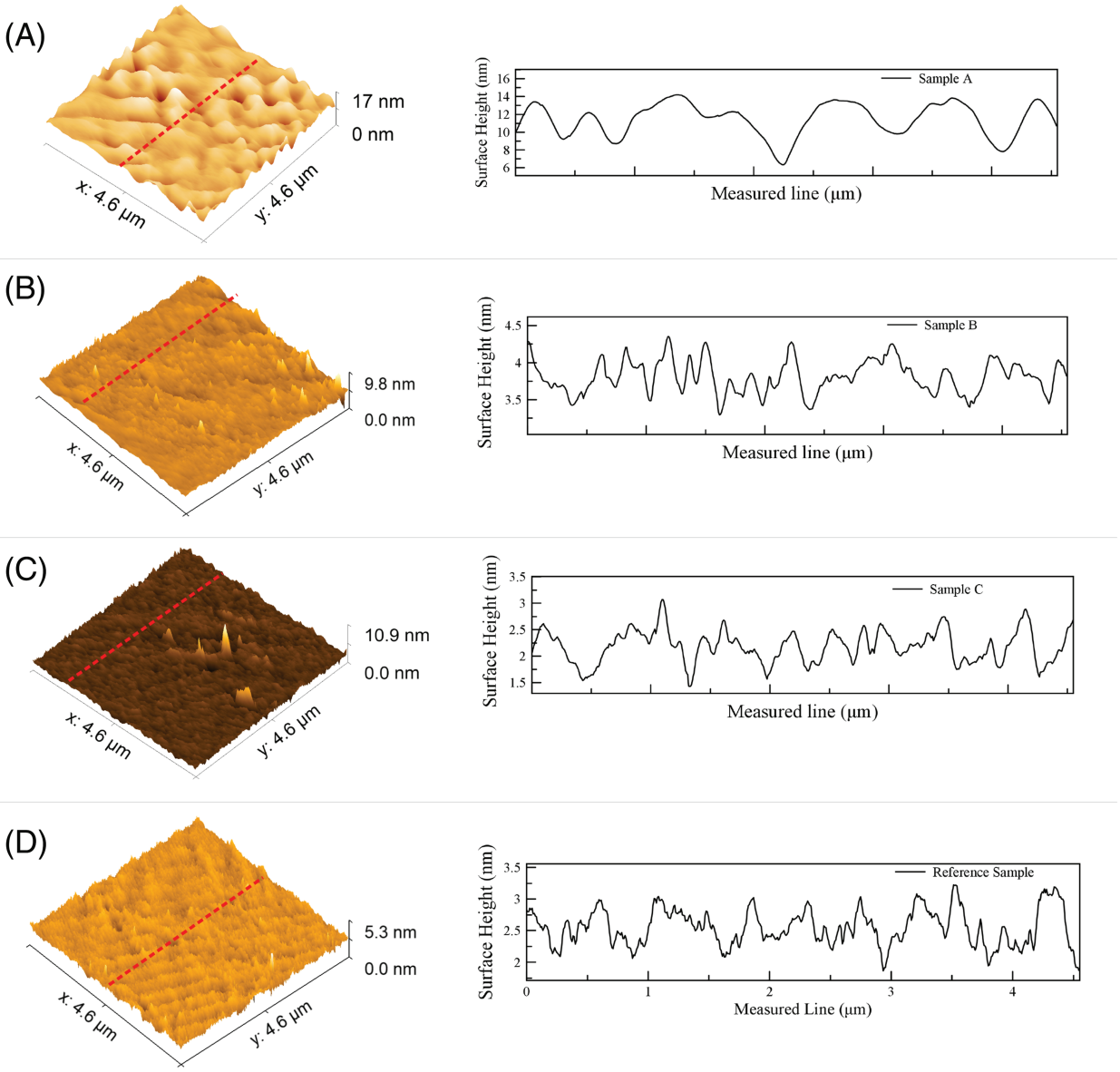

FIGURE 5 Atomic force microscopy (AFM) images and surface profiles (4.6 × 4.6 μm^2 scan area) of Samples (A) A, (B) B, (C) C, and (D) reference sample (red lines represent surface profile on AFM images)

TABLE 4 The critical and grown barrier layer thicknesses of the studied samples

Samples	Grown barrier layer thickness (nm)	Critical thickness (nm)	RMS (nm)
A	4	~6.4	1.52
B	3	Lattice-matched	0.34
C	3	~6.4	0.44
Reference	1	Lattice-matched	0.27

Abbreviation: RMS, root mean square values.

4 | CONCLUSION

The structural investigations of the AlN/GaN and the $In_{0.17}Al_{0.83}N$/GaN heterostructures with ultrathin barriers have been carried out via XRD and AFM measurements. The FWHM values and the dislocation densities of each sample were calculated. The sample with a lattice-matched $In_{0.17}Al_{0.83}N$ barrier (#sample B) was determined as the structure with the best structural quality concerning other studied samples. Sample B of the studied samples is shown lowest dislocation density with 1.69 × 10^8 cm^{-2}. The surface roughness of the studied

samples is found 0.27 nm as lowest value for reference sample. The increasing dislocation densities with the increasing barrier layer thicknesses are observed in the structures with the AlN barriers. In addition to this, the AlN interlayer is found to increase the dislocation density of the reference sample. For the studied samples, the edge dislocation density is more dominant than the screw dislocation density. Using the AlN interlayer is affected by the dislocation density and the surface roughness of InAlN/GaN heterostructure. AFM images are shown that an increment in the thickness of the AlN barrier layer gives rise to the relaxation of strain. These results are very crucial to determine optimum AlN barrier layer thickness in GaN-based heterostructures.

ACKNOWLEDGMENTS

SBL was supported in part by the Distinguished Young Scientist Award of the Turkish Academy of Sciences (TUBA-GEBIP 2016). EO acknowledges partial support from the Turkish Academy of Sciences (TUBA). We would like to thank Bilkent University NANOTAM engineers for their help.

ORCID

Polat Narin https://orcid.org/0000-0003-3956-7277

REFERENCES

1. Nakamura N, Furuta K, Shen XQ, et al. Electrical properties of MBE-grown AlGaN/GaN HEMT structures by using 4H-SiC (0001) vicinal substrates. *J Cryst Growth*. 2007;301-302:452-456.
2. Meneghesso G, Meneghini M, Rossetto I, et al. Reliability and parasitic issues in GaN-based power HEMTs: a review. *Semicond Sci Technol*. 2016;31(9):093004.
3. Yu H, Caliskan D, Ozbay E. Growth of high crystalline quality semi-insulating GaN layers for high electron mobility transistor applications. *J Appl Phys*. 2006;100(3):033501.
4. Lytvyn PM, Kuchuk AV, Mazur YI, et al. Polarization effects in graded AlGaN nanolayers revealed by current-sensing and Kelvin probe microscopy. *ACS Appl Mater Inter*. 2018;10(7):6755-6763.
5. Zhang H, Huang C, Song K, et al. Compositionally graded III-nitride alloys: building blocks for efficient ultraviolet optoelectronics and power electronics. *Rep Prog Phys*. 2021;84(4):044401.
6. Brubaker MD, Genter KL, Roshko A, et al. UV LEDs based on p–i–n core–shell AlGaN/GaN nanowire heterostructures grown by N-polar selective area epitaxy. *Nanotechnology*. 2019;30(23):234001.
7. Yatabe Z, Asubar JT, Hashizume T. Insulated gate and surface passivation structures for GaN-based power transistors. *J Phys D Appl Phys*. 2016;49(39):393001.
8. Bouveyron R, Charles MB. Growth by MOCVD of In (Ga) AlN alloys, and a study of gallium contamination in these layers under nitrogen and hydrogen carrier gas. *J Cryst Growth*. 2017;2017(464):105-111.
9. Saidi I, Mejri H, Baira M, Maaref H. Electronic and transport properties of AlInN/AlN/GaN high electron mobility transistors. *Superlattices Microstruct*. 2015;84:113-125.
10. Cheng J, Yang X, Sang L, et al. Growth of high quality and uniformity AlGaN/GaN heterostructures on Si substrates using a single AlGaN layer with low Al composition. *Sci Rep*. 2016;6(1):1-7.
11. Cao Y, Jena D. High-mobility window for two-dimensional electron gases at ultrathin AlN/GaN heterojunctions. *Appl Phys Lett*. 2007;90(18):182112.
12. Li Z, Li C, Peng D, et al. Growth of quaternary InAlGaN barrier with ultrathin thickness for HEMT application. *Superlattices and Microstruct*. 2018;118:213-220.
13. Ostermaier C, Pozzovivo G, Carlin J-F, et al. Ultrathin InAlN/AlN barrier HEMT with high performance in normally off operation. *IEEE Electron Device Lett*. 2009;30(10):1030-1032.
14. Tasli P, Sarikavak B, Atmaca G, Elibol K, et al. Numerical simulation of novel ultrathin barrier n-GaN/InAlN/AlN/GaN HEMT structures: Effect of indium-mole fraction, doping and layer thicknesses. *Physica B Condens Matter*. 2010;405(18):4020-4026.
15. Leszczynski M, Teisseyre H, Suski T, et al. Lattice parameters of gallium nitride. *Appl Phys Lett*. 1996;69(1):73-75.
16. Susilo N, Roumeliotis GG, Narodovitch M, et al. Accurate determination of polarization fields in (0 0 0 1) c-plane InAlN/GaN heterostructures with capacitance-voltage-measurements. *J Phys D Appl Phys*. 2018;51(48):485103.
17. Stanchu H, Auf der Maur M, Kuchuk AV, et al. Compositionally graded AlGaN nanostructures: strain distribution and X-ray diffraction reciprocal space mapping. *Cryst Growth des*. 2020;20(3):1543-1551.
18. Liubchenko OI, Kladko VP, Sabov TM, Dubikovskyi OV. X-ray analysis for micro-structure of AlN/GaN multiple quantum well systems. *J Mater Sci Mater*. 2019;30(1):499-507.
19. Ťapajna M, Kaun SW, Wong MH, et al. Influence of threading dislocation density on early degradation in AlGaN/GaN high electron mobility transistors. *Appl Phys Lett*. 2011;99(22):223501.
20. Hájek F, Hospodkova A, Hubik P, et al. Transport properties of AlGaN/GaN HEMT structures with back barrier: impact of dislocation density and improved design. *Semicond. Sci. Technol*. 2021;36(7):075016.
21. Marino FA, Faralli N, Palacios T, Ferry DK, Goodnick SM, Saraniti M. Effects of threading dislocations on AlGaN/GaN high-electron mobility transistors. *IEEE Trans Electron Devices*. 2010;57(1):353-360.
22. Hentschel R, Gärtner J, Wachowiak A, Großer A, Mikolajick T, Schmult S. Surface morphology of AlGaN/GaN heterostructures grown on bulk GaN by MBE. *J Cryst Growth*. 2018;500:1-4.
23. Zhang AP, Rowland LB, Kaminsky EB, et al. Correlation of device performance and defects in AlGaN/GaN high-electron mobility transistors. *J Electron Mater*. 2003;32(5):388-394.
24. Jabbari I, Baira M, Maaref H, Mghaieth R. Cryogenic investigation of the negative pinch-off voltage Vpinch-off, leakage current and interface defects in the $Al_{0.22}Ga_{0.78}N$/GaN/SiC HEMT. *Microelectron Reliab*. 2021;116:114009.
25. Hao Y, Yang LA, Zhang JC. GaN-based semiconductor devices for terahertz technology. *Terahertz Sci Tech*. 2008;1(2):51-64.
26. Jang SH, Lee CR. High-quality GaN/Si (1 1 1) epitaxial layers grown with various $Al_{0.3}Ga_{0.7}N$/GaN superlattices as intermediate layer by MOCVD. *J Cryst Growth*. 2003;253(1–4):64-70.
27. Sohi P, Martin D, Grandjean N. Critical thickness of GaN on AlN: impact of growth temperature and dislocation density. *Semicond Sci Technol*. 2017;32(7):075010.
28. Vispute RD, Talyansky V, Trajanovic Z, et al. High quality crystalline ZnO buffer layers on sapphire (001) by pulsed laser deposition for III–V nitrides. *Appl Phys Lett*. 1997;70(20):2735-2737.
29. Rathkanthiwar S, Kalra A, Muralidharan R, Nath DN, Raghavan S. Growth of AlN on sapphire: predicting the optimal nucleation density by surface kinetics modeling. *J Appl Phys*. 2020;127(20):205301.
30. Bai J, Wang T, Comming P, Parbrook PJ, David JPR, Cullis AG. Optical properties of AlGaN/GaN multiple quantum well structure by using a high-temperature AlN buffer on sapphire substrate. *J Appl Phys*. 2006;99(2):023513.
31. Tang B, Hu H, Wan H, et al. Growth of high-quality AlN films on sapphire substrate by introducing voids through growth-mode modification. *Appl Surf Sci*. 2020;518:146218.

32. Potì B, Tagliente MA, Passaseo A. High quality MOCVD GaN film grown on sapphire substrates using HT-AlN buffer layer. *J Non Cryst Solids*. 2006;352(23–25):2332-2334.
33. Sarikavak-Lisesivdin B, Lisesivdin SB, Ozbay E. The effect of InxGa1−xN back-barriers on the dislocation densities in Al0.31Ga0.69N/AlN/GaN/InxGa1−xN/GaN heterostructures (0.05 ≤ x ≤ 0.14). *Curr Appl Phys*. 2013;13(1):224-227.
34. Teke A, Gökden S, Tülek R, et al. The effect of AlN interlayer thicknesses on scattering processes in lattice-matched AlInN/GaN two-dimensional electron gas heterostructures. *New J Phys*. 2009;11(6):063031.
35. McAleese C, Kappers MJ, Rayment FDG, Cherns P, Humphreys CJ. Strain effects of AlN interlayers for MOVPE growth of crack-free AlGaN and AlN/GaN multilayers on GaN. *J Cryst Growth*. 2004;272(1–4):475-480.
36. Shen XQ, Takahashi T, Kawashima H, Ide T, Shimizu M. Realization of compressively strained GaN films grown on Si(110) substrates by inserting a thin AlN/GaN superlattice interlayer. *Appl Phys Lett*. 2012;101(3):031912.
37. Dunn CG, Kogh EF. Comparison of dislocation densities of primary and secondary recrystallization grains of Si-Fe. *Acta Metal*. 1957;5(10):548-554.
38. Zanato D, Gokden S, Balkan N, Ridley BK, Schaff WJ. The effect of interface-roughness and dislocation scattering on low temperature mobility of 2D electron gas in GaN/AlGaN. *Semicond Sci Technol*. 2004;19(3):427-432.
39. Tang H, Webb JB, Coleridge P, et al. Scattering lifetimes due to interface roughness with large lateral correlation length inAlxGa1−xN/GaNtwo-dimensional electron gas. *Phys Rev B*. 2002;66(24):245305.
40. Narin P, Arslan E, Ozturk M, Ozturk M, Lisesivdin SB, Ozbay E. Scattering analysis of ultrathin barrier (<7 nm) GaN-based heterostructures. *Appl Phys A*. 2019;125(4):1-7.
41. Skromme BJ, Zhao H, Wang D, et al. Strain determination in heteroepitaxial GaN. *Appl Phys Lett*. 1997;71(6):829-831.
42. Rinke P, Winkelnkemper M, Qteish A, Bimberg D, Neugebauer J, Scheffler M. Consistent set of band parameters for the group-III nitrides AlN, GaN, and InN. *Phys Rev B*. 2008;77(7):1-15.

How to cite this article: Narin P, Kutlu-Narin E, Atmaca G, Sarikavak-Lisesivdin B, Lisesivdin SB, Ozbay E. A structural analysis of ultrathin barrier (In)AlN/GaN heterostructures for GaN-based high-frequency power electronics. *Surf Interface Anal*. 2022;54(5):576-583. doi:10.1002/sia.7067